

Structural Determination of a Short-Lived Excited Iron(II) Complex by Picosecond X-Ray Absorption Spectroscopy

Wojciech Gawelda,^{1,2} Van-Thai Pham,¹ Maurizio Benfatto,³ Yuri Zaushitsyn,¹ Maik Kaiser,² Daniel Grolimund,² Steven L. Johnson,² Rafael Abela,² Andreas Hauser,⁴ Christian Bressler,^{1,*†} and Majed Chergui^{1,*‡}

¹*Ecole Polytechnique Fédérale de Lausanne, Laboratoire de Spectroscopie Ultrarapide, ISIC, FSB-BSP, CH-1015 Lausanne, Switzerland*

²*Paul Scherrer Institut, Swiss Light Source, CH-5232 Villigen PSI, Switzerland*

³*Laboratori Nazionali di Frascati, INFN, CP13, I-00044 Frascati, Italy*

⁴*Département de Chimie Physique, Université de Genève, 30 quai Ernest-Ansermet, CH-1121 Genève, Switzerland*

(Received 2 August 2006; published 2 February 2007)

Structural changes of the iron(II)-tris-bipyridine ($[\text{Fe}^{\text{II}}(\text{bpy})_3]^{2+}$) complex induced by ultrashort pulse excitation and population of its short-lived (≤ 0.6 ns) quintet high spin state have been detected by picosecond x-ray absorption spectroscopy. The structural relaxation from the high spin to the low spin state was followed over the entire lifetime of the excited state. A combined analysis of the x-ray-absorption near-edge structure and extended x-ray-absorption fine structure spectroscopy features delivers an Fe-N bond elongation of 0.2 Å in the quintet state compared to the singlet ground state.

DOI: 10.1103/PhysRevLett.98.057401

PACS numbers: 78.70.Dm, 82.40.-g, 82.53.Kp

Molecular iron(II) complexes exhibit strongly coupled electronic, magnetic, and structural dynamics. They have been extensively studied in relation to the phenomenon of spin crossover (SCO), where a transition from a low spin (LS) ground state to a high spin (HS) excited state is induced by either temperature or light [1], while the reverse transformation can be induced by pressure [2]. The study of SCO compounds is being actively pursued for potential applications in magnetic data storage and as a basis for bistable devices [3]. In biology, SCO plays an important role in the binding of ligands in heme proteins [4]. Finally, ultrafast spin changes (like the case presented here) may offer a route for data processing at the nanoscale [5].

A characteristic energy level scheme for iron(II) complexes is shown in Fig. 1. In compounds with a sufficiently low zero-point energy difference ΔE_{HL}^0 between LS and HS states, i.e., of the order of 100–1000 cm^{-1} , SCO can be temperature induced, but this is not possible for $[\text{Fe}^{\text{II}}(\text{bpy})_3]^{2+}$ with a $\Delta E_{\text{HL}}^0 \approx 6000$ cm^{-1} . The population of the HS state of Fe(II)-based SCO complexes can be triggered optically in the so-called light-induced excited spin state trapping (LIESST) process [1,6]. However, the lifetime of the HS state of $[\text{Fe}^{\text{II}}(\text{bpy})_3]^{2+}$ is limited to microseconds at cryogenic temperatures, in contrast to the light-induced HS state of SCO complexes with low-temperature lifetimes of more than 10 h. Photoexcitation of $[\text{Fe}^{\text{II}}(\text{bpy})_3]^{2+}$ by UV-visible light populates the singlet metal-to-ligand-charge-transfer ($^1\text{MLCT}$) states, and is followed by a cascade of intersystem crossing steps through MLCT and ligand-field (LF) states, which brings the system to its lowest-lying quintet state (HS), 5T_2 , with almost unit quantum yield within < 1 ps [7,8]. At room temperature, this state relaxes nonradiatively to the LS ground state in ~ 0.6 ns in aqueous solutions. Knowledge of the relationship between the HS \rightarrow LS relaxation rate,

ΔE_{HL}^+ , and the Fe-N equilibrium distance is crucial for the design of molecules with longer-lived HS states.

Steady-state structural studies on Fe(II) SCO compounds, both in the LS ground and the HS states generated by LIESST or temperature, have been carried out using x-ray crystallography and x-ray absorption spectroscopy (XAS), all delivering an elongation of the Fe-N bond by 0.18–0.22 Å, with respect to the LS ground state

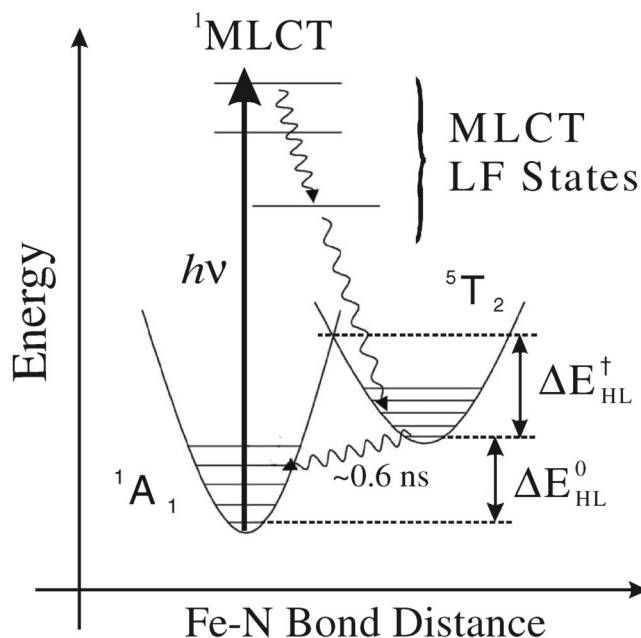


FIG. 1. Schematic potential energy curves of Fe(II)-SCO complexes as a function of the Fe-N bond distance, and pathways of nonradiative relaxation leading to the short-lived quintet state (0.6 ns for $[\text{Fe}^{\text{II}}(\text{bpy})_3]^{2+}$), upon excitation of the singlet MLCT state in the UV.

[9–21]. Recently, Fe K -edge steady-state XAS of the LS $[\text{Fe}(\text{tren}(\text{py})_3)](\text{PF}_6)_2$ and its HS analogue $[\text{Fe}(\text{tren}(6\text{-Me-py})_3)](\text{PF}_6)_2$ were combined to interpret the picosecond transient spectra of the photoactivated $[\text{Fe}(\text{tren}(\text{py})_3)](\text{PF}_6)_2$ complex, showing good agreement with the anticipated result for the HS complex [22].

This Letter presents a picosecond study at the Fe K -edge absorption of photoexcited aqueous $[\text{Fe}^{\text{II}}(\text{bpy})_3]^{2+}$. The key point here is that, contrary to LIESST-SCO complexes, for $[\text{Fe}^{\text{II}}(\text{bpy})_3]^{2+}$ picosecond XAS is the only possible method to determine the structural parameters of the light-induced HS state, because its lifetime is too short for quasistatic structural studies, even at the lowest temperatures. Here, we capture the structure of the short-lived HS intermediate ($\tau \leq 0.6$ ns), with 100 ps hard x-ray pulses, and map out the evolution of the structure over the entire HS lifetime. In addition, and contrary to previous work [22], we extract the structural parameters of the HS state directly from a fit of the experimental difference absorption spectra without prior assumptions about its structure. The structural parameters of the HS state were retrieved from both the x-ray absorption near edge structure (XANES) [23,24] and the extended x-ray absorption fine structure (EXAFS) [25], delivering identical results within their uncertainties.

The laser-pump x-ray-probe experiments were performed at the micro-XAS beam line of the Swiss Light Source. Details of the experimental strategy are described elsewhere [26–28]. Briefly, an intense 400 nm pulse (100 fs pulse width, repetition rate 1 kHz) excites an aqueous solution of 1–25 mM $[\text{Fe}^{\text{II}}(\text{bpy})_3]^{2+}$, while a ~ 100 ps monochromatic (0.016% bandwidth) tunable hard x-ray pulse probes the system by x-ray absorption spectroscopy as a function of the adjustable pump-probe time delay. The detected signal is the difference x-ray absorption spectrum between the laser excited and the unexcited sample, recorded on a shot-to-shot basis at 2 kHz. The XAS of the sample was measured in both transmission and x-ray fluorescence yield modes. The incident x-ray flux was monitored via x-ray fluorescence from a thin Cr foil placed upstream from the sample. The x-ray energy was calibrated via a reference spectrum of an iron foil.

For the quantitative structural analysis, we used two approaches. First, we implemented the MXAN code described in Refs. [23,24]. It uses the so-called full multiple scattering (FMS) approach, avoiding any *a priori* selection of the relevant multiple scattering paths, together with the muffin-tin approximation for the shape of the atomic potentials [29], which are recalculated and optimized at each step of the least-squares minimization procedure. Here, we use a recent extension of the MXAN code [30] to fit the difference x-ray absorption spectra in energy space, which is more sensitive for the structural analysis. In the second approach, we fitted the Fourier-transformed EXAFS spectra of the LS and HS spectra using the theoretical scattering amplitudes and phases delivered by the FEFF 8.2 code, after

applying the appropriate data reduction procedure to convert the spectra to wave vector space [31].

Figure 2(a) shows the static XAS spectrum of the first 200 eV of the Fe K absorption edge of $[\text{Fe}^{\text{II}}(\text{bpy})_3]^{2+}$. It is characterized by a number of XANES features (labeled A to D), whose assignments were already discussed in Refs. [16,32]. The resonances above ~ 50 eV from the edge are predominantly single scattering features (i.e., the EXAFS), in particular, feature E, which is dominated by scattering from the nearest N atoms. In XAS studies of similar compounds it was observed that all these features change drastically upon SCO [16,19–21], as seen in Fig. 2(b) for the transient absorption spectrum (50 ps after excitation) and in the reconstructed (as explained below) HS spectrum [Fig. 2(a)]. Most of the changes at the B to E bands are attributed to changes of metal-ligand and intra-ligand bond distances and angles, with the Fe-N bond being the dominant contributor. Additional changes in the high energy (EXAFS) region (not shown here) are also clearly observed, which likewise point to a significant

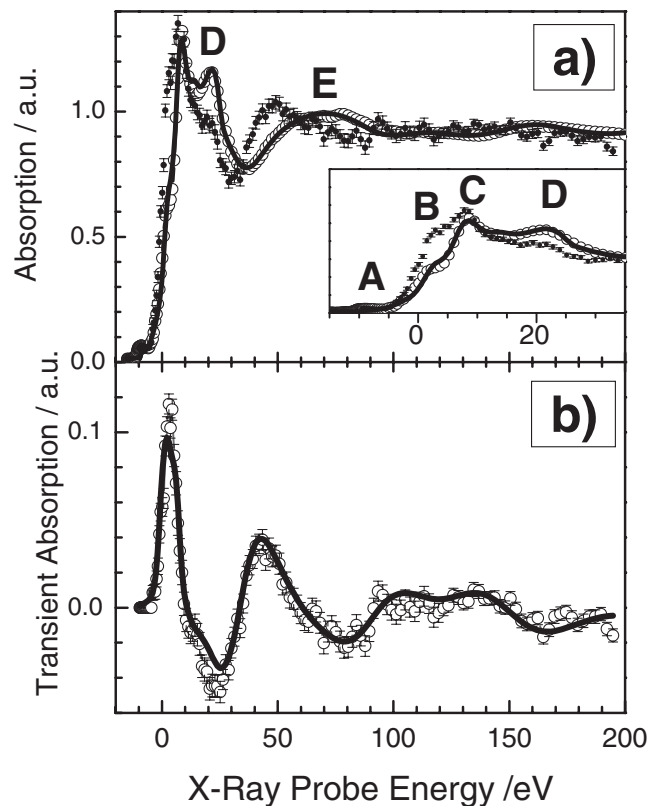


FIG. 2. (a) XANES spectrum of the LS state of a 25 mM aqueous solution of $[\text{Fe}^{\text{II}}(\text{bpy})_3]^{2+}$ (circles) and simulated MXAN spectrum (solid line) using an Fe-N bond distance of 2.0 Å. The inset shows details of the edge region and of the fit. The dots represent the XANES spectrum of the HS state retrieved via Eq. (1). The spectrum is plotted with respect to E_0 (7122.5 eV). (b) Experimental difference XANES recorded 50 ps after laser excitation (circles), and the fit results obtained by the FMS theory (solid line) with an Fe-N bond distance of 2.0 Å and a chemical shift of -2.5 eV (see text for details).

Fe-N bond change. Figure 3 compares the temporal evolution of the absorption changes at the B feature (7126 eV) with the kinetics of the ground state recovery measured by femtosecond optical pump-probe spectroscopy [8]. The latter reflects the repopulation of the LS state by the decay of the HS state and it matches the x-ray data perfectly.

Our results differ from previous XAS studies of light-induced SCO systems, which used exclusively the LIESST phenomenon in low-temperature solids to gain information about the structural characteristics of the HS state [16,18,20,21]. Also in Ref. [22], the detected HS complex in solution was relatively long-lived (60 ns), compared to the experimental resolution of the experiment (70 ps). Here, we impulsively photoinduce a transition to the HS state in a room temperature solution using a femtosecond laser pulse and follow the evolution of its electronic and structural properties over its entire sub-ns lifetime.

The difference absorption spectrum [Fig. 2(b)] is defined as [33]

$$\Delta A(E, \Delta t) = f(\Delta t)[A_{\text{HS}}(E, \Delta t) - A_{\text{LS}}(E)], \quad (1)$$

where $f(\Delta t)$ is the fractional population of the HS complex at time delay Δt [$= 50$ ps in Fig. 2(b)], $A_{\text{LS}}(E)$ is the absorption spectrum of the LS complex [Fig. 2(a)], and $A_{\text{HS}}(E, \Delta t)$ is that of the HS complex, at the time delay Δt after photoexcitation. In order to extract the excited state structure correctly, $f(\Delta t)$ must be known, and we measured a value of $22 \pm 2\%$ at $\Delta t = 50$ ps, in laser-only pump-probe experiments carried out under identical experimental conditions (laser fluence, sample concentration, and thick-

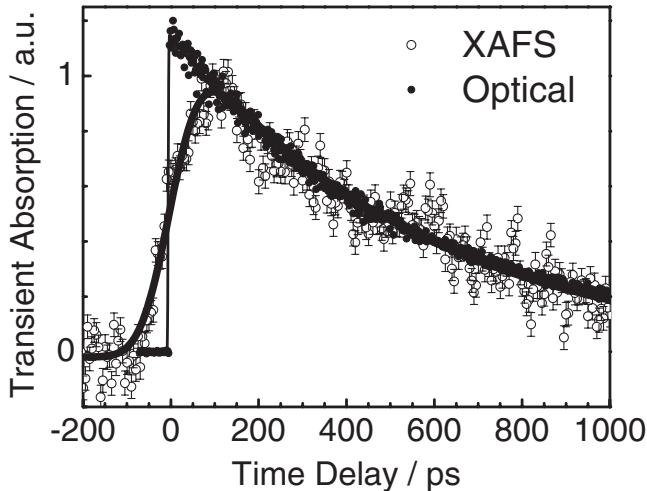


FIG. 3. Kinetics of the difference x-ray absorption fine structure (XAFS) signal of aqueous $[\text{Fe}^{\text{II}}(\text{bpy})_3]^{2+}$ at room temperature, recorded at 7126 eV (circles) upon 400 nm excitation, and that of the optical signal (dots) recorded in transmission at 523 nm, both reflecting the population of the excited state. The solid lines represent monoexponential fit curves with a decay constant of 650 ps. In the case of the x-ray signal, convolution with the 100 ps width of the x-ray pulse was included. Both spectra and fit curves are normalized to half-height of the rise.

ness) as in the x-ray experiments. The fractional HS population was estimated from the bleach of the ground state absorption upon 400 nm excitation [8], taking into account the unit quantum yield for populating the quintet state [7]. The recovered HS state XAS spectrum is shown in Fig. 2(a).

For the structural analysis, we start off by fitting the XANES spectrum of the LS ground state using the MXAN code [Fig. 2(a)], as a check of the initial parameters. The fit [Fig. 2(a)] agrees very well with the experimental spectrum, including the edge region (see inset), delivering an Fe-N bond length of $R_{\text{Fe-N}} = 2.00 \pm 0.02 \text{ \AA}$, in good agreement with crystallographic data ($1.967 \pm 0.006 \text{ \AA}$) [34] and density functional theory (DFT) calculations ($1.99 \pm 0.02 \text{ \AA}$) [35]. Next, we fit the difference spectrum [Fig. 2(b)] to extract the Fe-N bond distances in the HS state. This is done by simulating the XANES spectrum of the HS state for varying Fe-N bond distances, and taking the difference with the LS state. However, the bond changes also modify the electronic structure, affecting both the edge features (A and B), the ionization potential $E_0 = 7122.5 \text{ eV}$, and features C, D, and E, above it. This is rationalized by the chemical shift, which represents the shift of the ionization potential E_0 of the Fe atom, due to the bond length changes in the HS state. E_0 is critical for the structural determination. Since its shift is not known *a priori*, we carried out a Monte Carlo optimization of the fit by minimization of the square residual function [30], which measures the quality of the agreement between the experimental and simulated traces. In the first optimization, we took the experimental photoexcitation yield of 22%, and obtained a chemical shift $\Delta E_0 = -2.5 \pm 0.5 \text{ eV}$ and an Fe-N bond elongation of $\Delta R_{\text{Fe-N}} = 0.20 \pm 0.05 \text{ \AA}$. As a confirmation, we then fixed ΔE_0 to -2.5 eV and repeated the optimization with $f(\Delta t = 50 \text{ ps})$ as adjustable parameter, yielding $f(\Delta t = 50 \text{ ps}) = 20\% - 23\%$ and $\Delta R_{\text{Fe-N}} = 0.19 \pm 0.03 \text{ \AA}$. The resulting fit curve is presented in Fig. 2(b), showing good agreement with the experimental difference spectrum.

Finally, we also fitted the k^3 -weighted EXAFS spectra of the LS and HS complexes using the scattering amplitudes and phases obtained with the FEFF 8.20 code. Figure 4 shows a comparison of the Fourier-transformed experimental and fitted spectra (not corrected for the central atom phase shift, which corresponds to 0.3 \AA). The fits were obtained using the first-shell contribution only and both LS and HS Fe-N bond distances were freely optimized in the fits (restrained to all 6 N atoms having the same bond distance). The LS bond distance is $1.99 \pm 0.02 \text{ \AA}$, while for the HS state we find $R_{\text{HS}} = 2.19 \pm 0.04 \text{ \AA}$, i.e., $\Delta R_{\text{Fe-N}} = 0.2 \pm 0.02 \text{ \AA}$, fully consistent with the above MXAN results. Important in the EXAFS fit is the value of the chemical shift, since it determines the value of the photoelectron wave vector. We optimized it independently and obtained a value of $\Delta E_0 = -2.8 \pm 0.5 \text{ eV}$ for the HS state, which agrees remarkably well with the MXAN result.

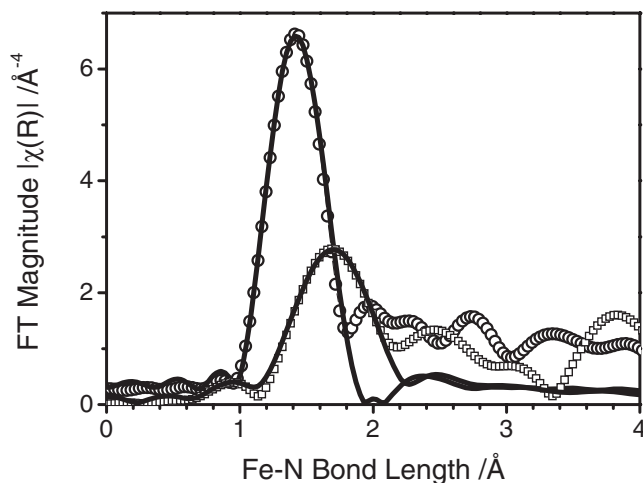


FIG. 4. Fourier Transforms (FT) of k^3 -weighted EXAFS spectra of the LS (circles) and HS (squares) complexes together with their fits (solid lines) using a first-shell model with 6 nearest neighbor N atoms (FT magnitudes are not phase corrected; therefore, they appear at shorter bond lengths).

The $\Delta R_{\text{Fe-N}}$ values of ~ 0.2 Å extracted from both the XANES and the EXAFS are in very good agreement with the LS-to-HS bond elongation from DFT calculations on $[\text{Fe}^{\text{II}}(\text{bpy})_3]^{2+}$ [35], and with the values derived for other Fe(II)-based SCO complexes using time resolved [22] and static structural methods [9–18,20,21]. That the bond elongation is nearly the same for all complexes, despite their largely different HS lifetimes, confirms the fact that the driving force for the HS-LS relaxation is determined by the energetics of the HS state, rather than its structure [36].

The time scale for the relaxation steps from the singlet $^1\text{MLCT}$ to the HS state is subpicosecond [8]. Optical spectroscopy is unable to resolve them, as they are spectroscopically silent [8]. Future extensions using femtosecond x-ray pulses extracted from a synchrotron, using the so-called “slicing” scheme [37], will soon provide insight into these steps and the structural changes therein occurring.

This work was funded by the Swiss National Science Foundation (FNRS), via Contracts No. 620-066145, No. 200021-107956, and No. 200021-105239. We thank M. Willimann, M. Harfouche, and B. Meyer for their assistance and help during the measurements.

*Corresponding author.

†Electronic address: Christian.Bressler@epfl.ch

‡Electronic address: Majed.Chergui@epfl.ch

- [1] P. Gütllich, A. Hauser, and H. Spiering, *Angew. Chem., Int. Ed. Engl.* **33**, 2024 (1994).
 [2] V. Ksenofontov, A. B. Gaspar, and P. Gütllich, in *Spin Crossover in Transition Metal Compounds III*, Topics in

- Current Chemistry Vol. 235, edited by P. Gütllich and H. A. Goodwin (Springer, Berlin, 2004), p. 23.
 [3] J. F. Letard, P. Guionneau, and L. Goux-Capes, in *Spin Crossover in Transition Metal Compounds III* (Ref. [2]), p. 221.
 [4] J. N. Harvey, *Faraday Discuss.* **127**, 165 (2004).
 [5] G. P. Zhang *et al.*, in *Spin Dynamics in Confined Magnetic Structures I*, Topics in Applied Physics Vol. 83, edited by B. Hillebrands and K. Ounadjela (Springer, Berlin, 2002), p. 245.
 [6] A. Hauser, in *Spin Crossover in Transition Metal Compounds II*, Topics in Current Chemistry Vol. 234, edited by P. Gütllich and H. A. Goodwin (Springer, Berlin, 2004), p. 234.
 [7] C. Brady *et al.*, in *Spin Crossover in Transition Metal Compounds III* (Ref. [2]), p. 1
 [8] W. Gawelda *et al.*, *J. Am. Chem. Soc.* (to be published).
 [9] J. Kusz, H. Spiering, and P. Gütllich, *J. Appl. Crystallogr.* **34**, 229 (2001).
 [10] E. J. MacLean *et al.*, *Chem. Eur. J.* **9**, 5314 (2003).
 [11] J. Kusz *et al.*, *J. Appl. Crystallogr.* **38**, 528 (2005).
 [12] A. L. Thompson *et al.*, *Chem. Commun. (Cambridge)* **12** (2004) 1390.
 [13] K. Okamoto *et al.*, *Chem. Phys. Lett.* **371**, 707 (2003).
 [14] P. Guionneau *et al.*, in *Spin Crossover in Transition Metal Compounds II* (Ref. [6]), p. 97.
 [15] M. Hostettler *et al.*, *Angew. Chem., Int. Ed. Engl.* **43**, 4589 (2004).
 [16] C. Hannay *et al.*, *Inorg. Chem.* **36**, 5580 (1997).
 [17] P. J. van Koningsbruggen *et al.*, *Inorg. Chem.* **39**, 1891 (2000).
 [18] T. Yokoyama *et al.*, *Phys. Rev. B* **58**, 14 238 (1998).
 [19] M. L. Boillot *et al.*, *New J. Chem.* **26**, 313 (2002).
 [20] H. Oyanagi, T. Tayagaki, and K. Tanaka, *J. Phys. Chem. Solids* **65**, 1485 (2004).
 [21] H. Oyanagi, T. Tayagaki, and K. Tanaka, *J. Lumin.* **119**, 361 (2006).
 [22] M. Khalil *et al.*, *J. Phys. Chem. A* **110**, 38 (2006).
 [23] M. Benfatto *et al.*, *J. Synchrotron Radiat.* **8**, 267 (2001).
 [24] M. Benfatto *et al.*, *Phys. Rev. B* **65**, 174205 (2002).
 [25] A. L. Ankudinov *et al.*, *Phys. Rev. B* **58**, 7565 (1998).
 [26] M. Saes *et al.*, *Rev. Sci. Instrum.* **75**, 24 (2004).
 [27] W. Gawelda *et al.*, *Phys. Scr.* **T115**, 102 (2005).
 [28] W. Gawelda *et al.*, *J. Am. Chem. Soc.* **128**, 5001 (2006).
 [29] T. A. Tyson *et al.*, *Phys. Rev. B* **46**, 5997 (1992).
 [30] M. Benfatto *et al.*, *J. Phys. Chem. B* **110**, 14 035 (2006).
 [31] B. K. Teo, *EXAFS: Basic Principles and Data Analysis* (Springer, Berlin, 1986).
 [32] V. Briois *et al.*, *Inorg. Chem.* **40**, 912 (2001).
 [33] C. Bressler and M. Chergui, *Chem. Rev.* **104**, 1781 (2004).
 [34] S. Dick, *Z. Kristallogr. New Cryst. Struct.* **213**, 356 (1998).
 [35] L. M. L. Daku *et al.*, *Chem. Phys. Chem.* **6**, 1393 (2005).
 [36] A. Hauser, N. Amstutz, S. Delahaye, S. Schenker, A. Sadki, R. Sieber, and M. Zerara, in *Optical Spectra and Chemical Bonding in Inorganic Compounds*, Structure and Bonding Vol. 106, edited by Th. Schönher (Springer, Berlin, 2003), p. 81.
 [37] R. W. Schoenlein *et al.*, *Science* **287**, 2237 (2000).